Electronic Supplementary Information for

Structural change induced by electrochemical sodium extraction from layered O'3-$NaMnO_2$

Kei Kubota,[ab] Masahiro Miyazaki,[a] Eun Jeong Kim,[a] Hiroaki Yoshida,[a] Prabeer Barpanda [c] and Shinichi Komaba*[ab]

[a.] *Department of Applied Chemistry, Tokyo University of Science, 1-3 Kagurazaka, Shinjuku-ku, Tokyo 162-8601, Japan.*
[b.] *Elements Strategy Initiative for Catalysts and Batteries (ESICB), Kyoto University, 1-30 Goryo-Ohara, Nishikyo-ku, Kyoto 615-8245, Japan.*
[c.] *Faraday Materials Laboratory, Materials Research Center, Indian Institute of Science, C.V. Raman Avenue, Bangalore, 560012, India.*

Table S1. Rietveld refinement results for as-prepared α-$NaMnO_2$.

R_{wp} = 8.37%, R_e = 3.99%

1st phase: 95.4 mass%
Space group: *C*2/*m*
a = 5.6644(1) Å, *b* = 2.8755(5) Å, *c* = 5.7996(2) Å, *β* = 113.153(2)°, *V* = 86.313(3) Å^3
R_B = 1.66%, R_F = 0.85%

Atom	Wyckoff site	*x*	*y*	*z*	*g*	*B* / Å^2
Na	2c	0	0	1/2	0.948(4)	0.31(5)
Mn	2b	0	1/2	0	1	0.39(2)
O	6c	0.2059(4)	0	0.2032(4)	1	0.52(4)

2nd phase: 4.6 mass%
Space group: *Pmmn*
a = 2.856(1) Å, *b* = 4.803(1) Å, *c* = 6.317(2) Å, *V* = 86.66(5) Å^3
R_B = 4.72%, R_F = 1.28%

Atom	Wyckoff site	*x*	*y*	*z*	*g*	*B* / Å^2
Na	4a	1/4	3/4	0.127(7)	1.0	0.90
Mn	2b	1/4	3/4	0. 623(3)	1.0	0.23
O1	2a	1/4	1/4	0.131(8)	1.0	0.50
O2	2a	1/4	1/4	0.557(7)	1.0	0.50

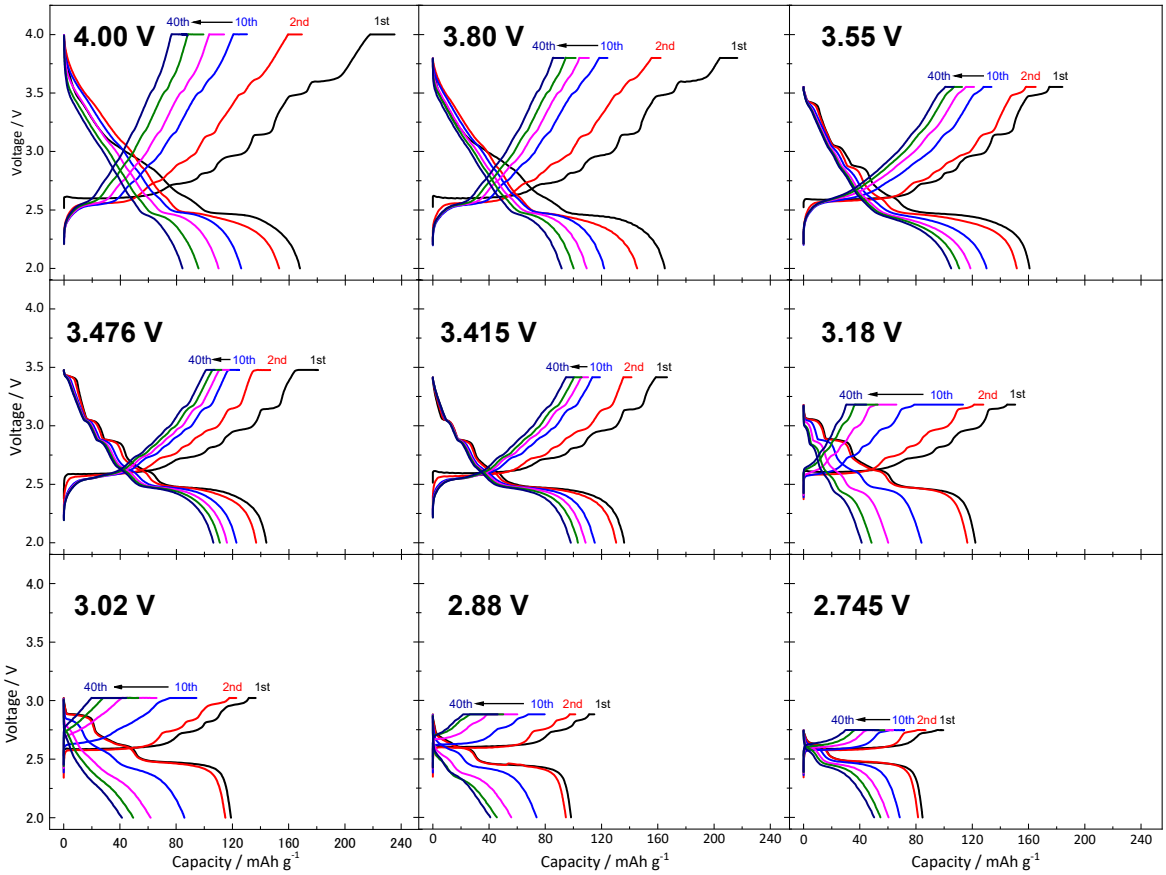

Figure S1. Charge-discharge curves of O'3-$NaMnO_2$ electrode in a Na cell cycled by charging to the different upper cut-off voltages in CC-CV mode and discharging to 2.0 V in CC mode at 12 mA g^{-1} at 25 °C.

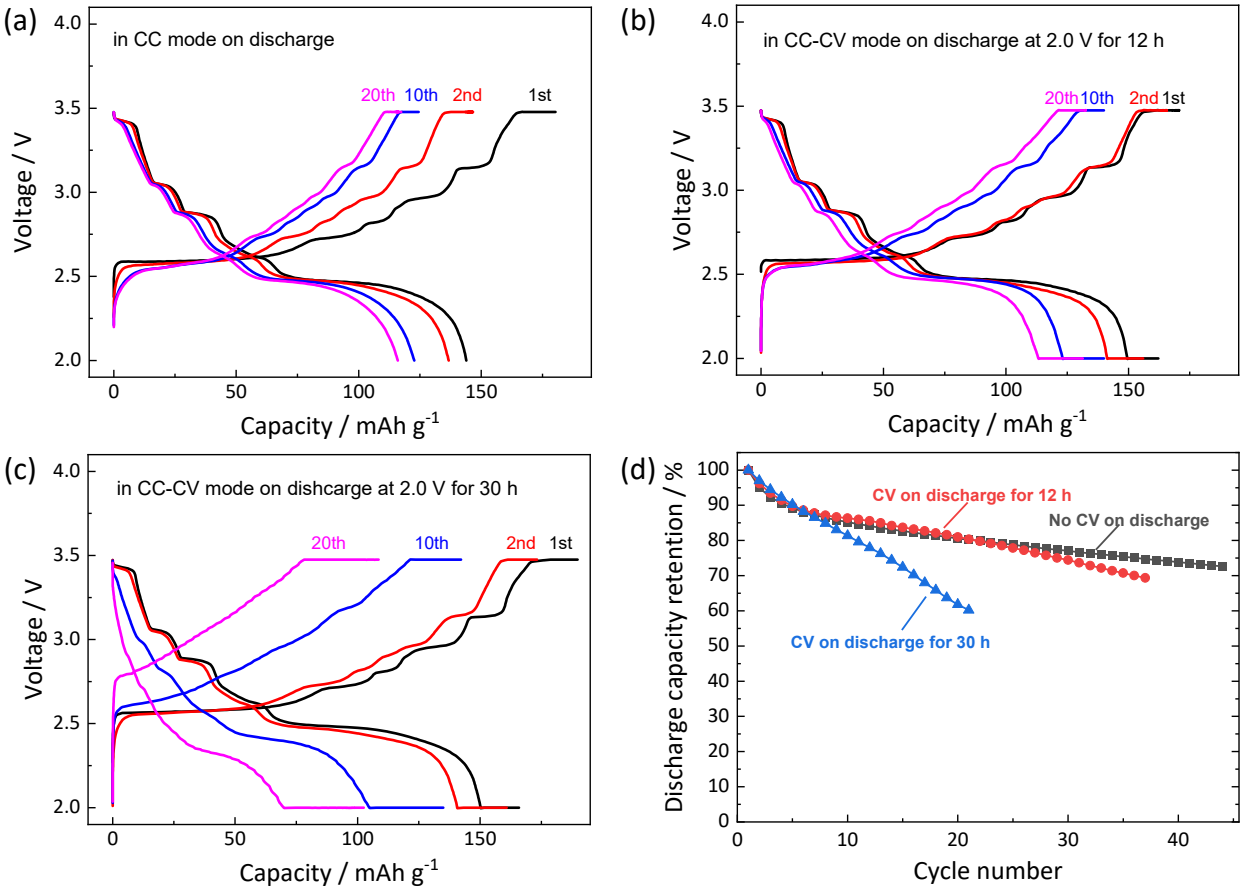

Figure S2. Charge-discharge curves of O'3-$NaMnO_2$ electrode in a Na cell cycled in CC-CV mode in the voltage range of 2.0–3.476 V at 12 mA g^{-1} at 25 °C. In addition to the 12 hrs holding at 3.476 V at the end of charging, holding for (a) 0, (b) 12, and (c) 30 h was applied at 2.0 V at the end of discharging. (d) Capacity retention rate during cycles.

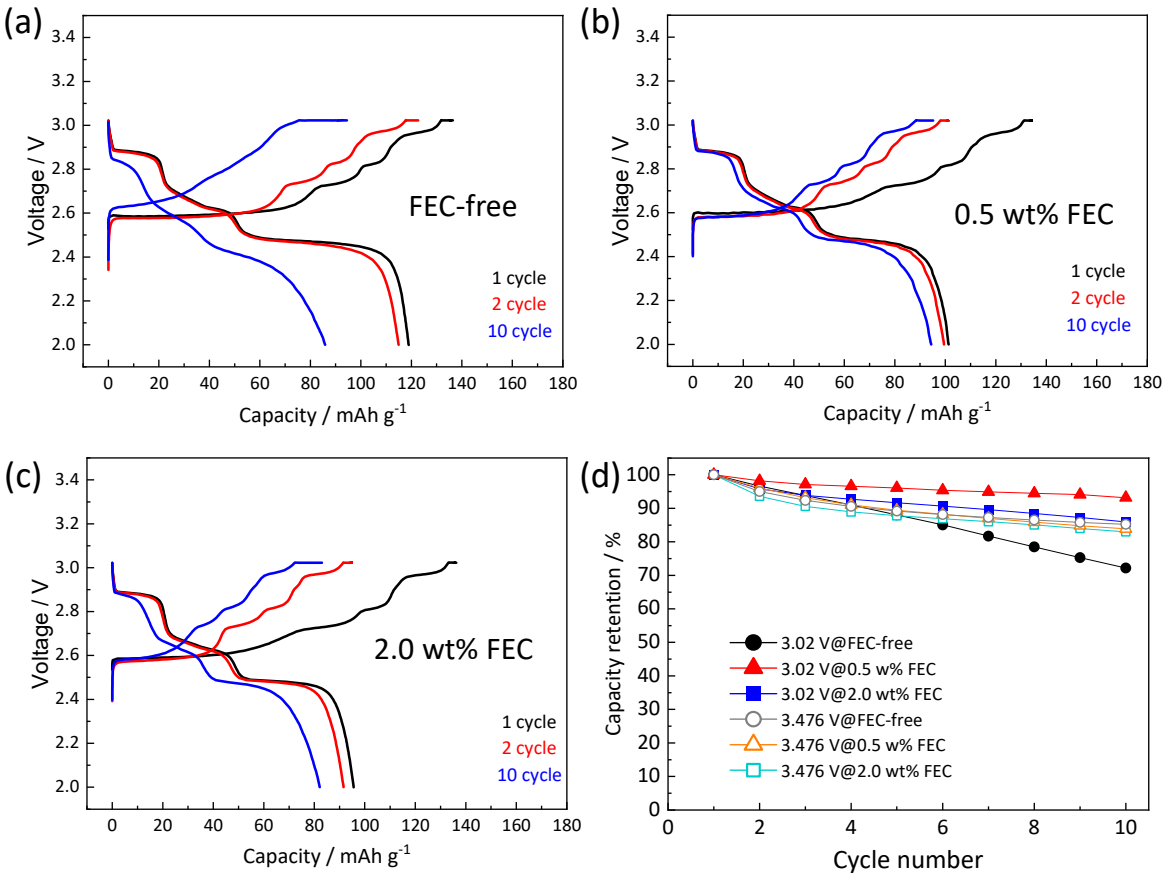

Figure S3. Charge and discharge curves of O'3-$NaMnO_2$ electrodes in Na cells filled with 1 mol dm^{-3} $NaPF_6$/PC electrolyte (a) without and with (b) 0.5 wt% or (c) 2.0 wt% fluoroethylene carbonate (FEC) as an electrolyte additive. Cells were cycled in 2.0–3.02 V at 25 °C charging under CC-CV mode at 12 mA g^{-1} and 12 hrs holding at 3.02 V on charging. (d) Cycle retention of the cells without and with FEC compared to cycling at 2.0–3.476 V.

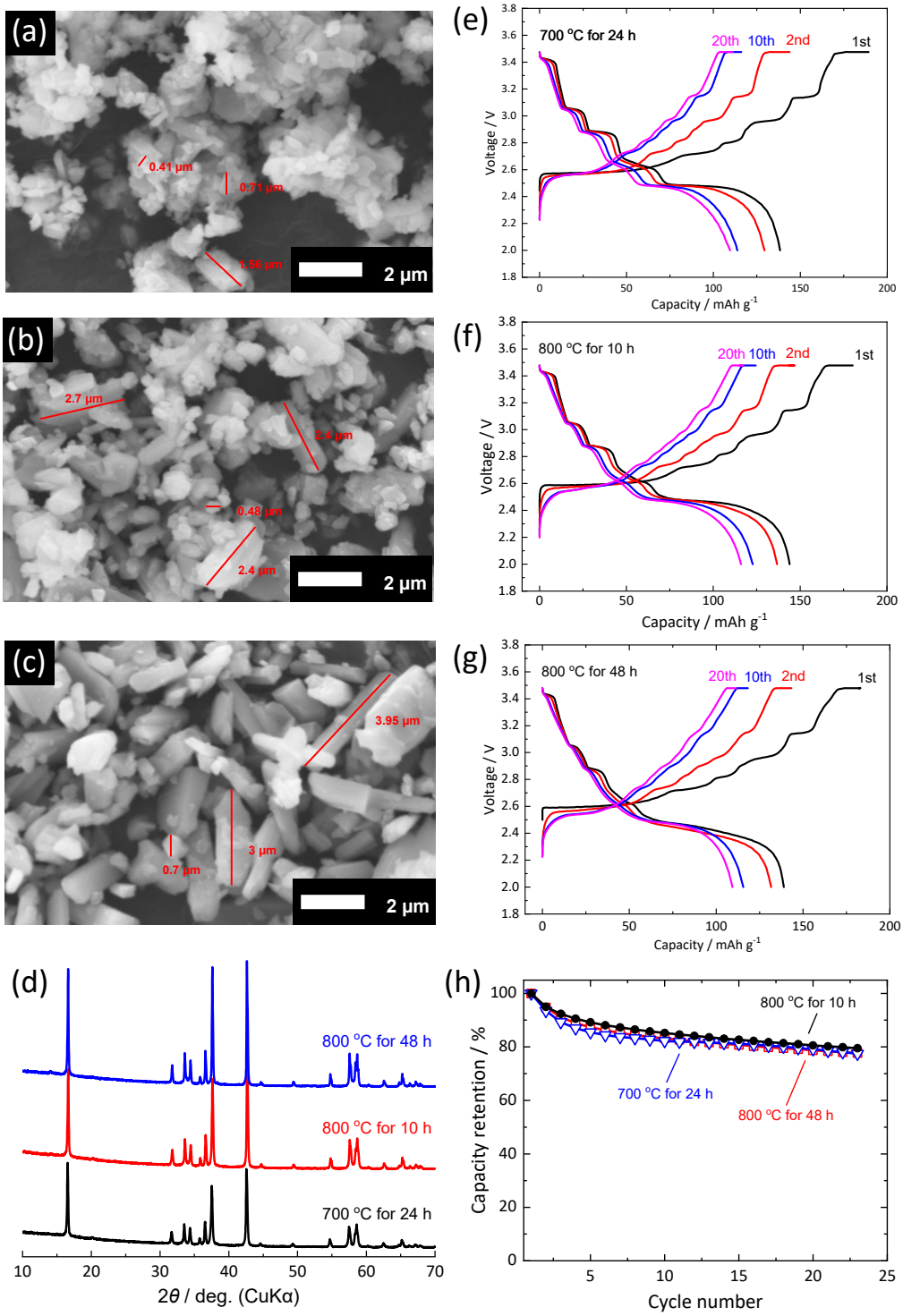

Figure S4. (a-c) SEM images, (d) XRD patterns, and (e-g) charge-discharge curves for O'3-$NaMnO_2$ prepared by heating at (a, e) 700 °C for 24 h, (b, f) 800 °C for 10 h, and (c, g) 800 °C for 48 h. (h) Capacity retention for the O'3-$NaMnO_2$ samples prepared through different heat-treatment temperature and time. Cells were cycled in 2.0–3.476 V at 25 °C charging under CC-CV mode at 12 mA g^{-1} and 12 hrs holding at 3.476 V on charging.

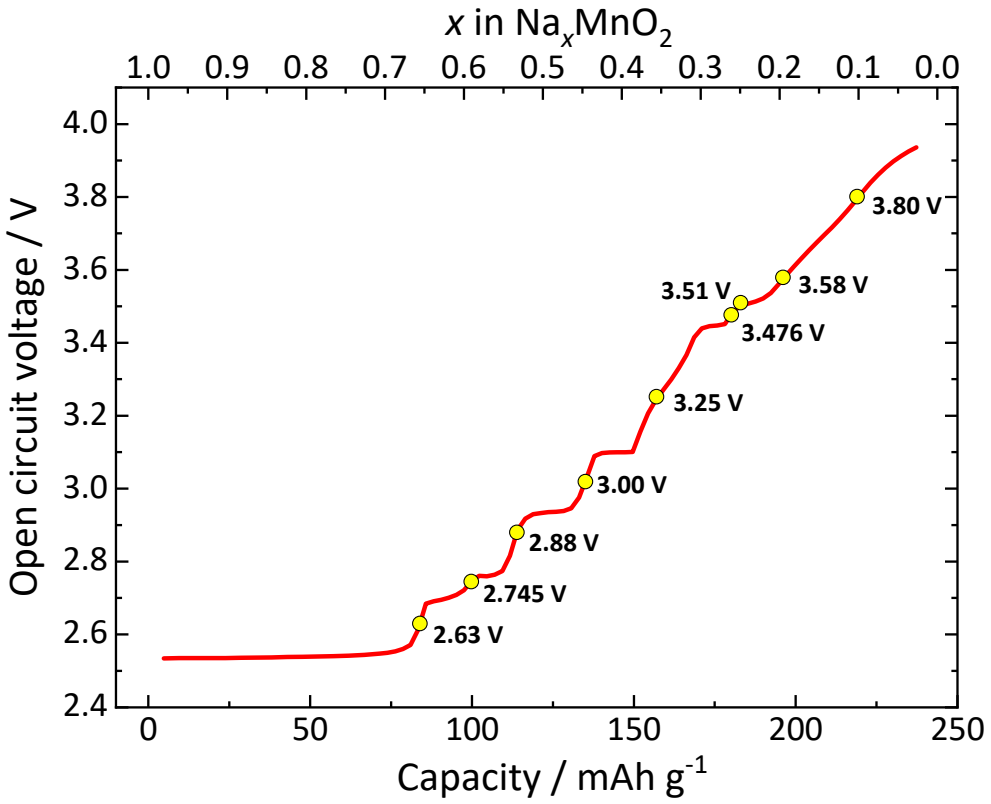

Figure S5. Open circuit voltage curve on the first charge obtained from GITT curves in Figure 3. Selected points for ex-situ synchrotron XRD measurements are indicated by yellow circles.

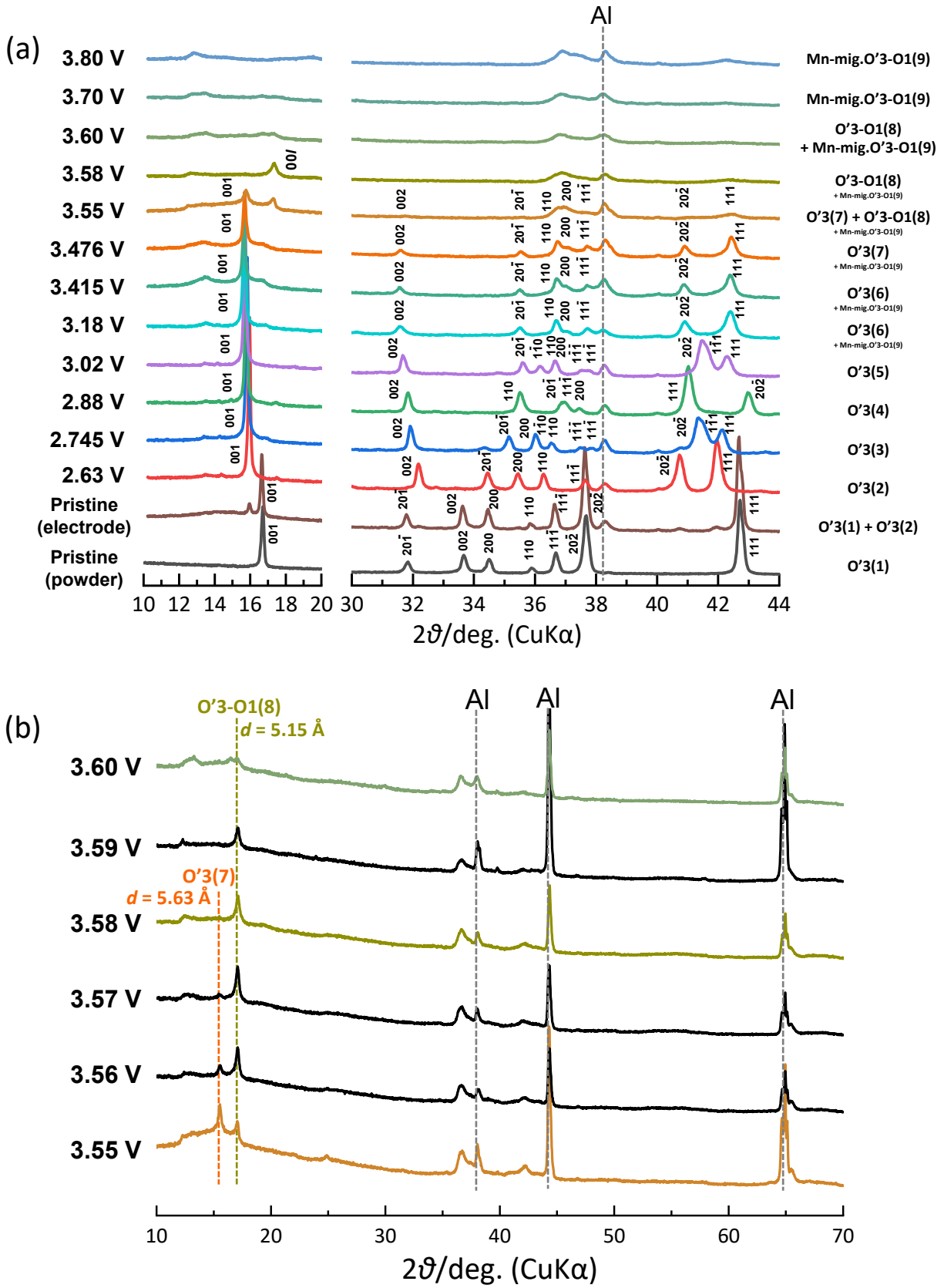

Figure S6. Laboratory-scale ex situ XRD patterns of the as-synthesized powder and the electrode samples of O'3-$NaMnO_2$ charged to various voltages; ranging (a) from 2.63 V to 3.80 V and (b) from 3.55 V to 3.60 V. The electrodes were prepared by galvanostatic charging at a current density of 12 mA g^{-1} followed by voltage holding at the targeted voltages for 60 hours.

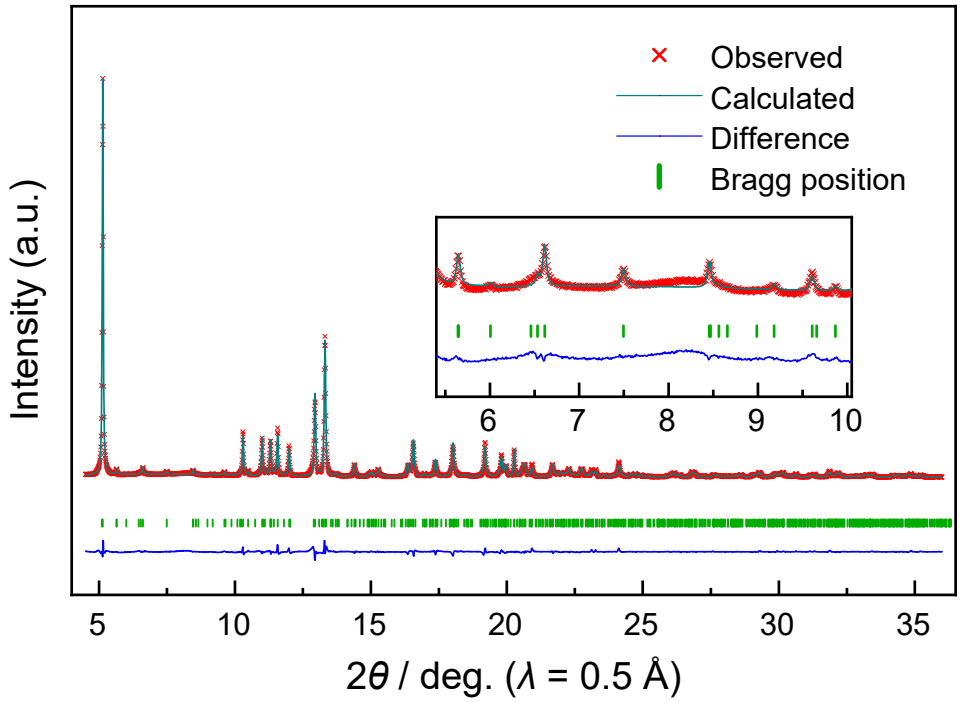

Figure S7. Rietveld refinement results for the ex-situ synchrotron XRD pattern of the electrode charged to 2.63 V. The refined structure corresponds to O'3(2) phase.

Table S2. Rietveld refinement results for the ex-situ synchrotron XRD pattern of the electrode charge to 2.63 V. The refined structure corresponds to O'3(2) phase.

R_{wp} = 7.01%, R_e = 4.34%
Space group: *C*2/*m*
a = 11.6151(4) Å, *b* = 5.6783(1) Å, *c* = 10.5199(3) Å, *β* = 105.356(2)°, *V* = 669.06(4) Å^3
R_B = 2.31%, R_F = 0.93%

Atom	Wyckoff site	*x*	*y*	*z*	*g*	*B* / Å^2
Na1	2c	0	0	1/2	0.80(2)	1.4(2)
Na2	4e	1/4	1/4	0	0.92(2)	= *B*(Na1)
Na3	4i	0.3959(9)	0	0.279(1)	0.99(2)	= *B*(Na1)
Na4	4i	= *x*(Na3) + 1/2	0	= *z*(Na3)	0.07(2)	= *B*(Na1)
Mn1	2a	0	0	0	1.0	0.34(3)
Mn2	2b	0	1/2	0	1.0	= *B*(Mn1)
Mn3	4i	0.2565(5)	0	0.4953(6)	1.0	= *B*(Mn1)
Mn4	8j	0.1407(2)	0.2501(8)	0.2458(3)	1.0	= *B*(Mn1)
O1	4i	0.189(2)	0	0.145(2)	1.0	0.44(9)
O2	4i	0.646(2)	0	0.120(2)	1.0	= *B*(O1)
O3	4i	0.599(2)	0	0.348(2)	1.0	= *B*(O1)
O4	4i	0.114(2)	0	0.410(1)	1.0	= *B*(O1)
O5	8j	0.312(1)	0.268(3)	0.410(1)	1.0	= *B*(O1)
O6	8j	0.4611(9)	0.243(2)	0.103(1)	1.0	= *B*(O1)

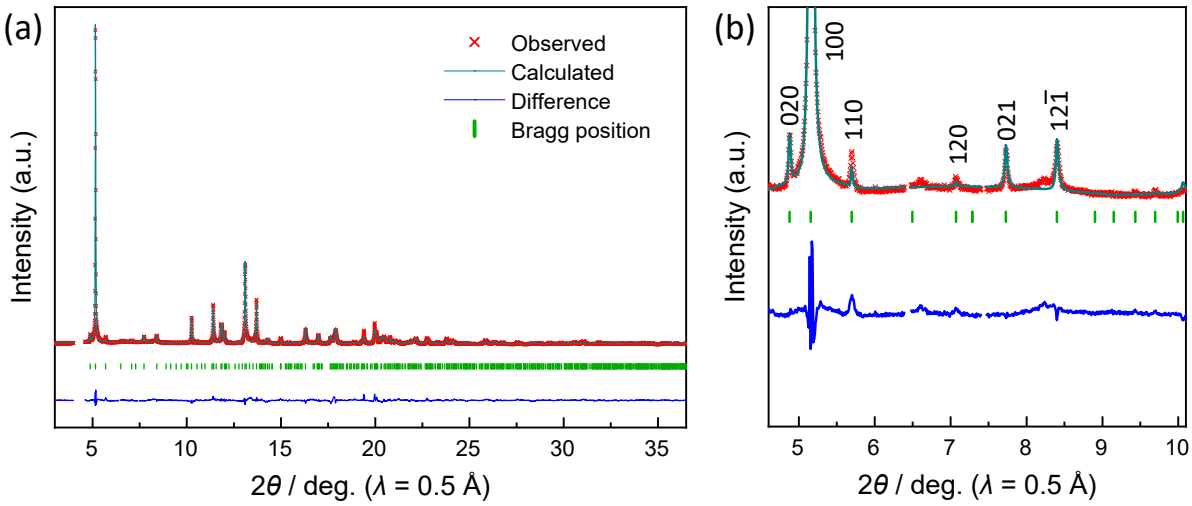

Figure S8. (a) Rietveld refinement results for the ex-situ synchrotron XRD pattern of the electrode charged to 2.88 V. (b) Magnified pattern in the diffraction angle of 5.5 – 10°. The refined structure corresponds to O'3(4) phase.

Table S3. Rietveld refinement results for the ex-situ synchrotron XRD pattern of the electrode charge to 2.88 V. The refined structure corresponds to O'3(4) phase.

R_{wp} = 11.54%, R_e = 3.85%
Space group: *P*2/*c*
a = 5.8118(3) Å, *b* = 11.9058(5) Å, *c* = 4.9629(3) Å, *β* = 104.480(4)°, *V* = 332.50(3) Å^3
R_B = 5.23%, R_F = 2.50%

Atom	Wyckoff site	*x*	*y*	*z*	*g*	*B* / Å^2
Na1	2f	1/2	0.172(2)	1/4	1.0	1.5
Na2	2f	1/2	0.677(2)	1/4	0.86(2)	= *B*(Na1)
Mn1	2e	0	0.0571(17)	1/4	1.0	0.6
Mn2	2e	0	0.3072(11)	1/4	1.0	= *B*(Mn1)
Mn3	2e	0	0.5653(17)	1/4	1.0	= *B*(Mn1)
Mn4	2e	0	0.8218(12)	1/4	1.0	= *B*(Mn1)
O1	4g	0.158(3)	0.427(3)	0.461(4)	1.0	0.8
O2	4g	0.155(6)	0.707(2)	0.461(9)	1.0	= *B*(O1)
O3	4g	0.175(5)	0.182(2)	0.485(7)	1.0	= *B*(O1)
O4	4g	0.253(3)	0.068(3)	0.037(4)	1.0	= *B*(O1)

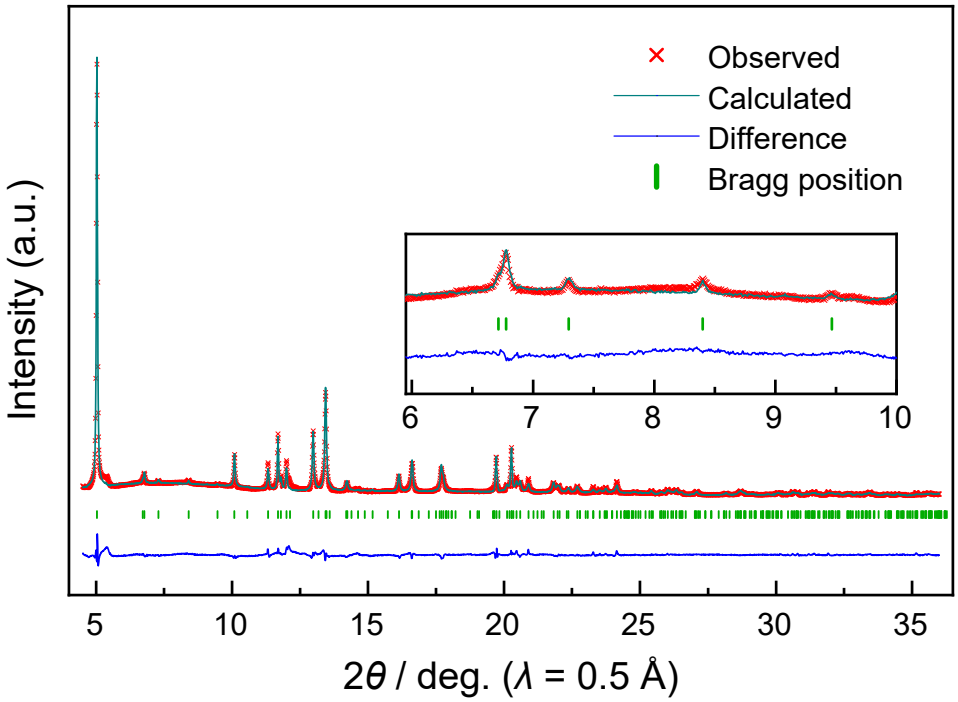

Figure S9. Rietveld refinement results for the ex-situ synchrotron XRD pattern of the electrode charged to 3.25 V. The refined structure corresponds to O'3(6) phase.

Table S4. Rietveld refinement results for the ex-situ synchrotron XRD pattern of the electrode charge to 3.25 V. The refined structure corresponds to O'3(6) phase.

R_{wp} = 7.48%, R_e = 3.14%
Space group: *C*2/*m*
a = 5.1023(4) Å, *b* = 8.5187(4), *c* = 5.9638(6) Å, *β* = 107.791(6)°, *V* = 246.82(3) Å^3
R_B = 7.33%, R_F = 3.93%

Atom	Wyckoff site	*x*	*y*	*z*	*g*	*B* / Å^2
Na1	2c	0	0	1/2	0.98(3)	1.7(4)
Na2	4h	0	1/3	1/2	0.06(2)	= *B*(Na1)
Mn1	2b	0	1/2	0	1.0	0.35(5)
Mn2	4g	0	0.166(1)	0	1.0	= *B*(Mn1)
O1	4i	0.200(4)	0	0.177(4)	1.0	1.2(1)
O2	8j	0.234(2)	1/3	0.172(2)	1.0	= *B*(O1)

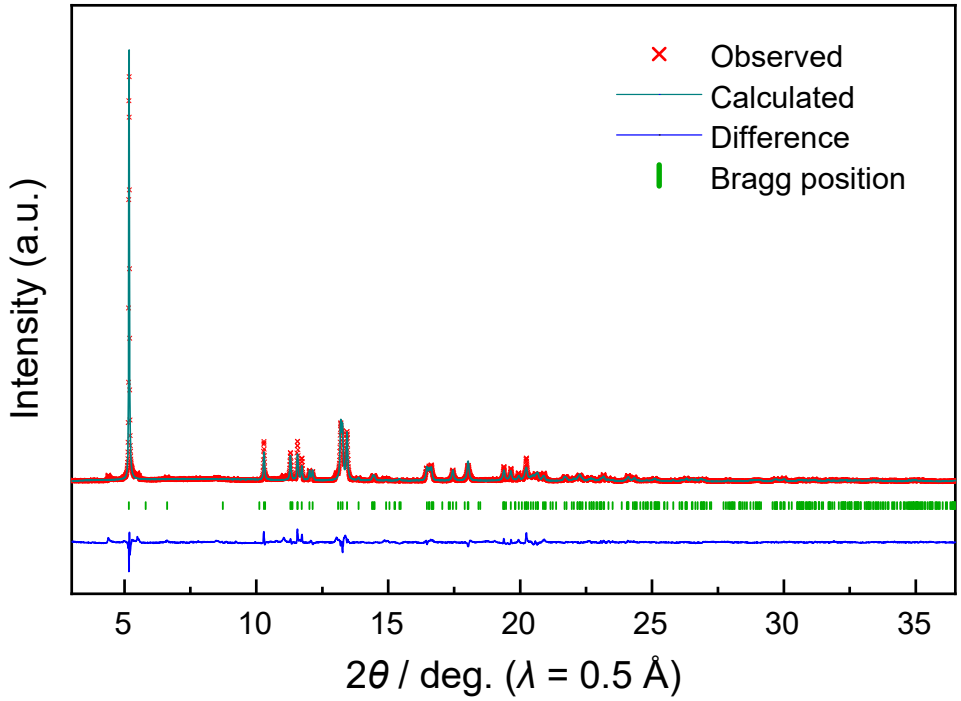

Figure S10. Rietveld refinement results for the ex-situ synchrotron XRD pattern of the electrode charged to 2.745 V. The refined structure corresponds to O'3(3) phase.

Table S5. Rietveld refinement results for the ex-situ synchrotron XRD pattern of the electrode charge to 2.745 V. The refined structure corresponds to O'3(3) phase.

R_{wp} = 14.33%, R_e = 3.90%
Space group: $P\bar{1}$

a = 5.1893(3) Å, b = 2.8521(1) Å, c = 5.8299(4) Å, α = 90.017(4)°, β = 105.873(5)°, γ = 90.865(4)°, V = 82.984(9) Å^3
R_B = 5.79%, R_F = 2.74%

Atom	Wyckoff site	x	y	z	g	B / Å^2
Na1	1f	1/2	0	1/2	0.45(3)	1.5
Na2	1g	0	1/2	1/2	0.39(1)	= B(Na1)
Mn1	1a	0	0	0	1.0	0.5
Mn2	1e	1/2	1/2	0	1.0	= B(Mn1)
O1	2i	0.715(3)	0.014(6)	0.157(1)	1.0	1.0
O2	2i	0.211(3)	0.491(6)	0.214(2)	1.0	= B(O1)

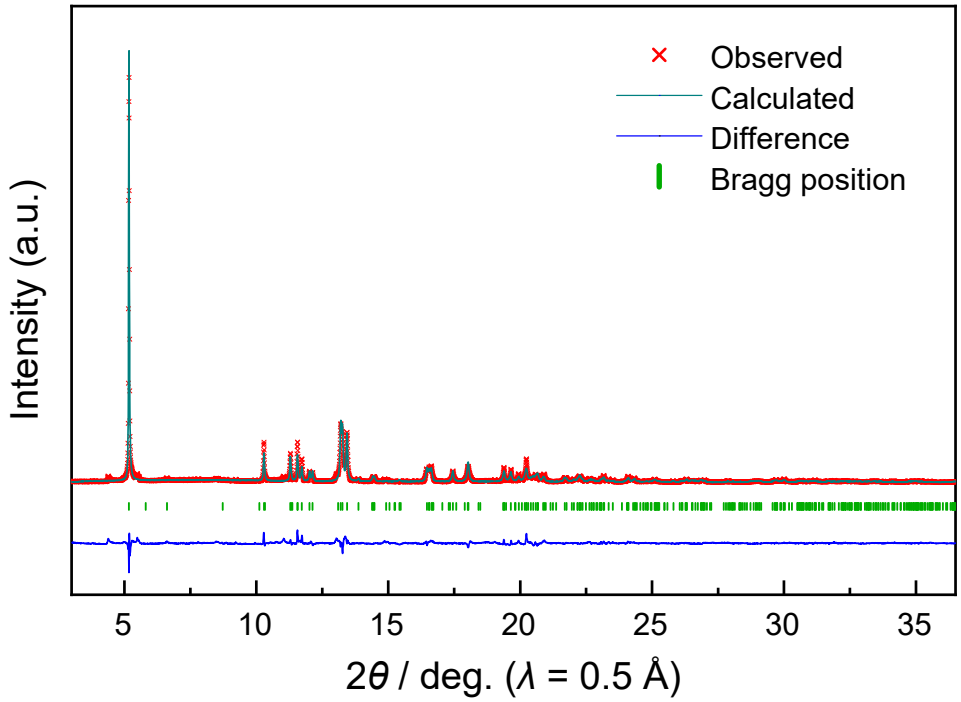

Figure S11. Rietveld refinement results for the ex-situ synchrotron XRD pattern of the electrode charged to 3.00 V. The refined structure corresponds to O'3(5) phase.

Table S6. Rietveld refinement results for the ex-situ synchrotron XRD pattern of the electrode charge to 3.00 V. The refined structure corresponds to O'3(5) phase.

R_{wp} = 7.53%, R_e = 2.93%
Space group: $P\bar{1}$

a = 5.1126(4) Å, b = 2.8592(2) Å, c = 5.8911(5) Å, α = 90.234(4)°, β = 106.305(5)°, γ = 90.787(4)°, V = 82.64(1) Å^3
R_B = 4.30%, R_F = 2.27%

Atom	Wyckoff site	x	y	z	g	B / Å^2
Na1	1f	0	1/2	1/2	0.50(2)	1.5
Na2	1g	1/2	0	1/2	0.25(2)	= B(Na1)
Mn1	1a	0	0	0	1.0	0.5
Mn2	1e	1/2	1/2	0	1.0	= B(Mn1)
O1	2i	0.712(6)	0.017(3)	0.163(2)	1.0	1.0
O2	2i	0.219(6)	0.482(3)	0.191(2)	1.0	= B(O1)

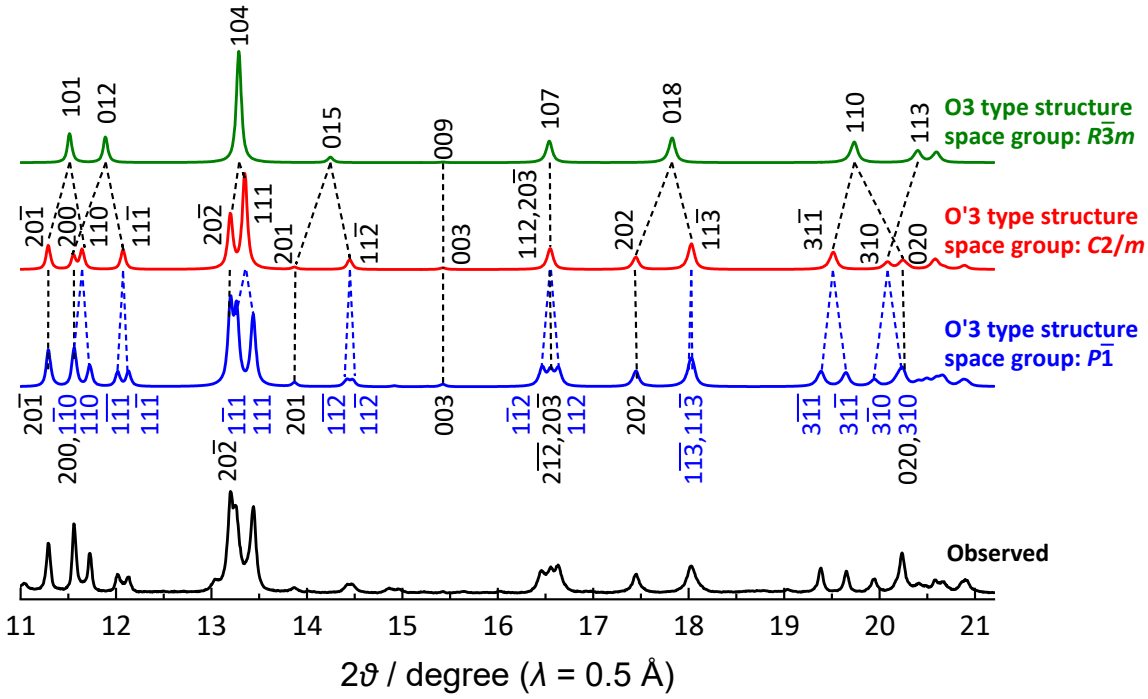

Figure S12. Observed synchrotron XRD pattern of the electrode charged to 2.745 V and simulated patterns for the three structures: rhombohedral O3 with space group of $R\bar{3}m$, monoclinic O'3 with $C2/m$, and triclinic O'3 with $P\bar{1}$. For rhombohedral O3 and monoclinic O'3 type structures, the composition used was $Na_{4/7}MnO_2$, whereas as-refined structural parameters, which were obtained through the Rietveld refinement of the XRD pattern of the electrode charged to 2.745 V (Figure S8 and Table S5), were used for the triclinic O'3 structure corresponding to O'3(3) phase.

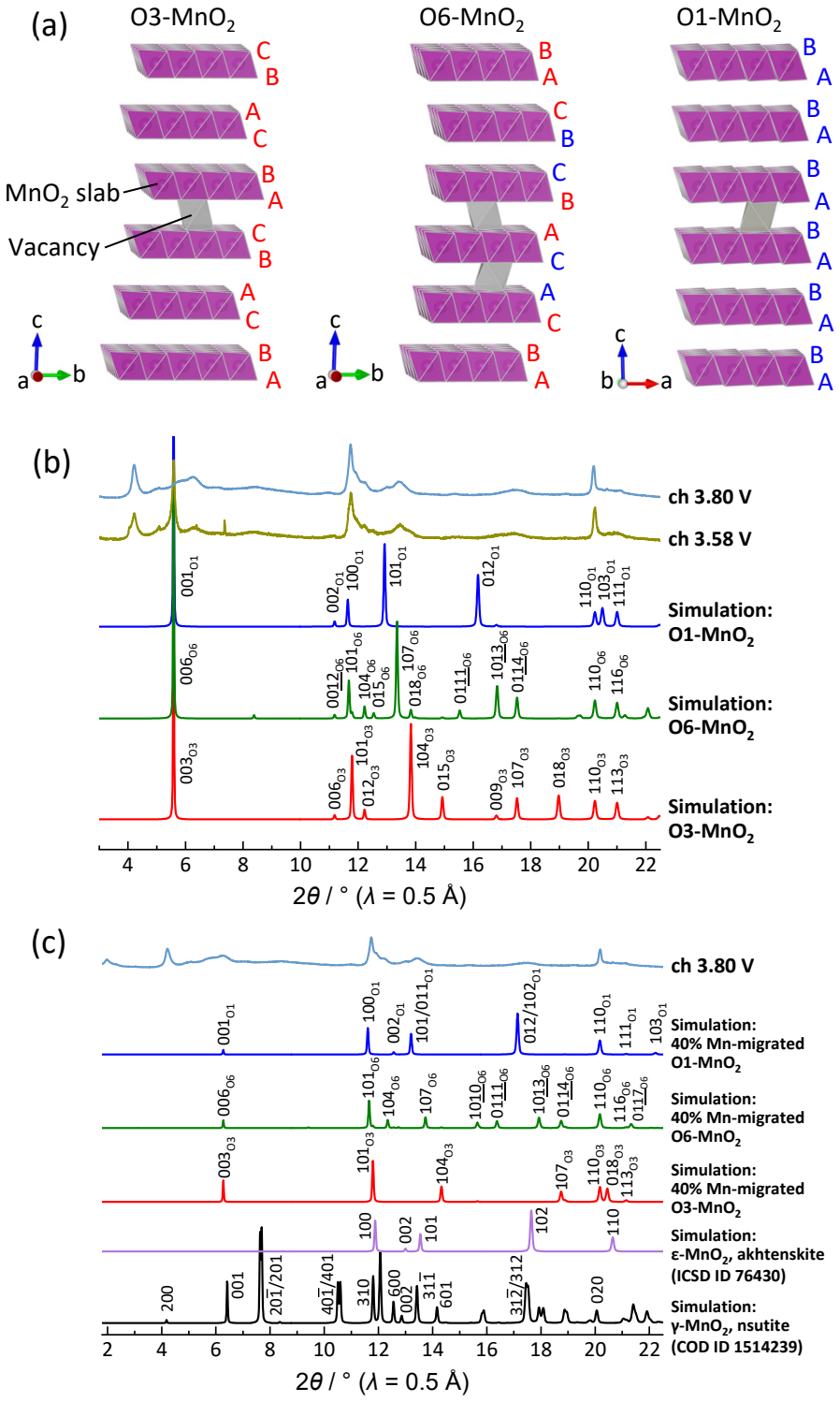

Figure S13. (a) Schematic illustrations of O3, O6, and O1 type MnO_2 structures. (b) ex situ XRD pattern for the electrodes charged to 3.58 and 3.80 V and the simulated patterns for the O3, O6, O1 type MnO_2 structures without migrated manganese ions. (c) ex situ synchrotron XRD pattern for the electrode charged to 3.80 V and the simulated patterns for the O3, O6, O1 type MnO_2 structures with 40% of migrated manganese ions from the MnO_2 slab to the vacant sodium sites in the interslab space. The sites to which the manganese ions migrate were considered to be tetrahedral sites in the O3 type interslab space and octahedral sites in the O1 type interslab space. Simulation patterns of γ- and ε-MnO_2 are also shown as a reference.

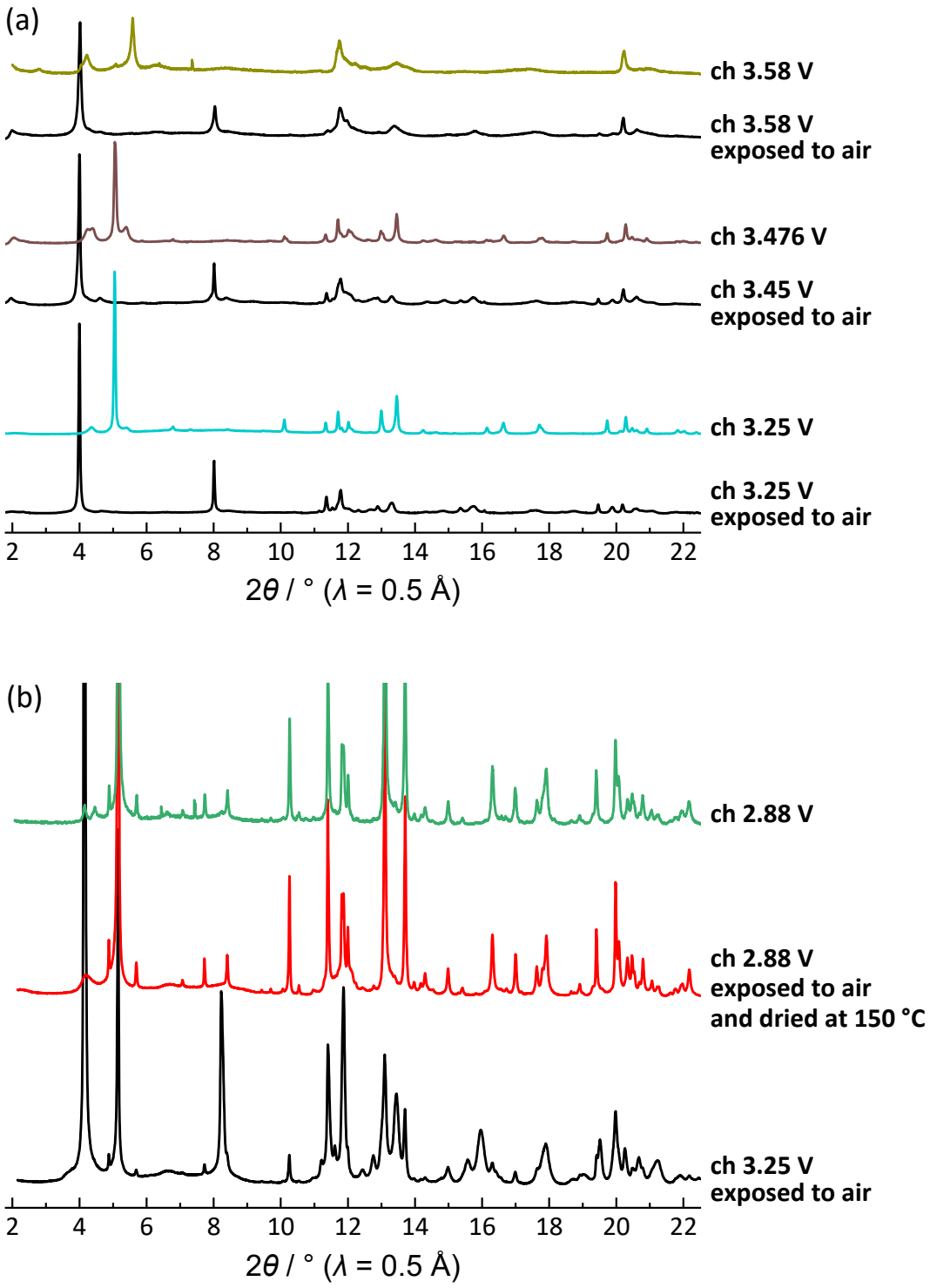

Figure S14. (a) ex situ synchrotron XRD patterns of the electrodes charged to 3.25, 3.476, and 3.58 V and those of the charged electrodes exposed to moist air due to failure to seal the capillary sample holder. The XRD patterns of hydrates often show diffraction peaks of 00*l* reflections at diffraction angles of about 4° and 8° at an X-ray wavelength of λ = 0.5 Å. (b) ex situ synchrotron XRD pattern of the electrode charged to 2.88 V and those of the electrodes exposed to moist air and dried at 150 °C. The patterns were collected at 20 °C.